Micromap Approach to Space Charge in a Synchrotron

G. Franchetti*†‡, I. Hofmann‡ and G. Turchetti*†

‡ *GSI, Plankstr. 1, D-64291, Darmstadt, Germany*
* *Dipartimento di Fisica, Universitá di Bologna, Via Irnerio 46, 40126, Bologna, Italy*
† *INFN, Sezione di Bologna, Via Irnerio 46, 40126, Bologna, Italy*

Abstract. A micromap approach to space charge is presented as a concept easily implemented in a computer code. A map of arbitrary length is found to be a suitable tool to include space charge by means of a kick approximation. We adopt space charge description where a transverse elliptic particle symmetry is assumed, and all analysis is carried out in a coasting beam approximation. This approach is particularly useful to investigate the single particle dynamics when the working point of a machine lies in a resonance driven by a skew quadrupole. Since the improvement of the multiturn injection efficiency due to linear coupling is based mainly on the exchange of emittance between x- and y- planes, we have investigated the emittance exchange dynamics when space charge is not negligible. We found that a coherent effect of space charge improves the efficiency of the exchange with respect to the case of single particle emittance exchange with space charge neglected.

I MICROMAP

We will describe the transverse dynamics of a single particle in a magnetic focusing lattice in a coordinate system where x, y denotes the horizontal and vertical axes perpendicular to the reference orbit ($x = y = 0$) and s is the axial (curvilinear) coordinate. The particle evolution in the horizontal $x - y$ plane is calculated as a function of s. In these coordinates the transverse equations of motion are

$$x'' - \left(k(s) - \frac{1}{\rho(s)^2}\right) x = \frac{1}{\rho(s)}\delta p + f_x(x, y, s) \tag{1a}$$

$$y'' + k(s)y = f_y(x, y, s) \tag{1b}$$

where $' = d/ds$, $k(s)$ is the quadrupole gradient, $\rho(s)$ is the $x-$plane radius of curvature of the reference orbit, δp is the off momentum, and $f_x(x, y, s)$ and $f_y(x, y, s)$ describe the nonlinearities of the applied focusing lattice [1].

In a linear lattice ($f_x = f_y = 0$) the solution of the Eq. (1) for the initial condition $\mathbf{x}(s) = (x, x^{'}, y, y^{'})_s$ can be expressed in terms of the transfer map

$$\mathbf{x}(s + \Delta s) = L_{s,s+\Delta s}\mathbf{x}(s) + \mathbf{D}_{s,s+\Delta s}\delta p \tag{2}$$

where $L_{s,s+\Delta s}$ is a block-diagonal matrix [1] and $\mathbf{D}_{s,s+\Delta s} = (D_{s,s+\Delta s}, D^{'}_{s,s+\Delta s})$ is a particular solution of Eq. (1a) corresponding to the initial condition $x(s) = 0$ and $x^{'}(s) = 0$.

If the lattice is not linear we can represent the effects of f_x, f_y in the dynamics while preserving the simplecticity of the transfer map Eq. (2) by using a single kick approximation [1]. The nonlinear effects on the particle moving in the interval $[s, s + \Delta s]$ are compressed in a kick $\mathbf{K}$ as follows

$$\mathbf{x}(s) \stackrel{\mathbf{K}}{\longmapsto} \mathbf{x}(s)^{'} \stackrel{\mathbf{L}}{\longmapsto} \mathbf{x}(s + \Delta s) \tag{3}$$

with $\mathbf{K}(\mathbf{x}) = (x, x^{'} + \Delta s f_x, y, y^{'} + \Delta s f_y)_s$. Therefore, the transfer map with kick approximation nonlinear forces is

$$\mathbf{x}(s + \Delta s) = L_{s,s+\Delta s} \begin{pmatrix} x \\ x^{'} + \Delta s f_x \\ y \\ y^{'} + \Delta s f_y \end{pmatrix}_s + \mathbf{D}_{s,s+\Delta s}\delta p \tag{4}$$

Validity of this method requires that the space step Δs be chosen consistently with the strengths of f_x and f_y and how they change with s.

In order to include space charge effects in the transverse map given by Eq. (4) using the single kick approximation, we have to evaluate the space charge contribution $f_{\zeta,sc}$ to the functions f_x and f_y (here $\zeta = x, y$). If we consider a particle moving in a drift, its equation of motion is

$$\frac{dp_\zeta}{dt} = F_{\zeta,sc} \tag{5}$$

It is straightforward to show that the relative error ΔA between dp_ζ/dt and $m\gamma_0(dv_\zeta/dt)$ is less then $(\gamma_0^2 - 1)(x^{'\,2} + y^{'\,2})$ where $\gamma_0 = (1 - \beta_0^2)^{-1/2}$. Using the parameters of the SIS ring [2], $\epsilon_x = 200$ mm mrad, $\epsilon_y = 20$ mm mrad, $\gamma_{xmax} = 0.86$, $\gamma_{ymax} = 1.98$, $\beta_{xmax} = 16.46$, $\beta_{ymax} = 28.52$, and $\beta_0 = 0.155$, we find that $\Delta A < 5.2 \cdot 10^{-3}$. Here we have denoted the $x-$ and $y-$plane emittances as ϵ_x and ϵ_y, $\gamma_{x,y\ max}$ and $\beta_{x,y\ max}$ denote the maximum values of the $x-$ and $y-$plane γ and beta functions describing the particle orbits, and β_0 is the relativistic factor of the design particle.

For such parameters Eq. (5) is well approximated as

$$\zeta^{''} = f_{\zeta,sc} \tag{6}$$

where $f_{\zeta,sc} = qE_{\zeta,sc}/v_0 p_0 \gamma_0^2$, q is the electric charge of the particle, $E_{\zeta,sc}$ is the space charge electric field, v_0 and p_0 are the axial velocity and momentum of the design

particle, and γ_0^2 represents the leading order correction to the electric force law due to self-magnetic fields.

The final form of the transverse micromap with space charge kicks is

$$\mathbf{x}(s+\Delta s) = L_{s,s+\Delta s} \begin{pmatrix} x \\ x' + \Delta s(f_{x,nl} + \frac{qE_x}{v_0 p_0 \gamma_0^2}) \\ y \\ y' + \Delta s(f_{y,nl} + \frac{qE_y}{v_0 p_0 \gamma_0^2}) \end{pmatrix}_s + \mathbf{D}_{s,s+\Delta s}\delta p \tag{7}$$

The evolution of an off-momentum particle in the step Δs is obtained by using the micromap in Eq. (7)

In order to include the effect of the bend frame, the axial space step Δs is related to the time step Δt by means of the formula

$$\Delta s = \frac{1}{1 + \frac{\mathcal{D}}{\rho}\delta p} v \Delta t$$

where v is the axial velocity of the particle, ρ the radius of curvature of the bend, and $\mathcal{D}$ is the dispersion function [3]. Note that each particle moves a different axial Δs for a fixed timestep.

II COASTING BEAM MODEL

A Macroparticle Description

In a coasting beam model with elliptic symmetry the particle density has the form

$$n(x, y, s) = n(\phi)$$

where ϕ is the isodensity parameter $\phi = x^2/a_x^2 + y^2/a_y^2$, and a_x, a_y are the rms transverse radii of the beam. Fig. 1 shows the scheme followed to introduce a macroparticle description of the coasting beam. We fix a series of transverse planes separated a distance dL from each other (Fig. 1a). Then we concentrate the particles between two successive planes as a macroparticle distribution on a single transverse plane as shown in Fig. 1b. We choose, arbitrarily, to put each of the macroparticles accumulation planes at the end of the accumulation interval. Each of the macroparticles has mass M^* and charge q^*. If n is the particle density of the coasting beam, the two dimensional particle density on a macroparticle plane α is $\delta = n \cdot dL$.

We can fill the transverse macroparticles planes of the beam with a sufficient number N^* of macroparticles to preserve the initial transverse symmetry of the beam. Since we have chosen to keep the macroparticle distribution on planes separated by a distance dL, it is also reasonable to keep the same average inter-particle

distance dL_α in the transverse direction. From this assumption we find a relation between N^* and dL

$$dL = \sqrt{\frac{\pi AB}{N^*}}$$

where $A = 2a_x$ and $B = 2a_y$. These assumptions determine the charge q^* and mass M^* of the macroparticles.

B Space Charge Calculation

The symmetry of the beam allows us to calculate the transverse component of the elettrostatic space charge electric field and the longitudinal component is zero by assumption. We assume free boundary condition. The transverse electric field components are given by the formulas [4]

$$E_x = \frac{q^*}{\epsilon_0} M_x x; \quad E_y = \frac{q^*}{\epsilon_0} M_y y$$

where

$$M_u = \frac{a_x a_y}{2} \int_0^\infty \frac{n(\lambda) ds}{(a_u^2 + s)\sqrt{(a_x^2 + s)(a_y^2 + s)}} \tag{8}$$

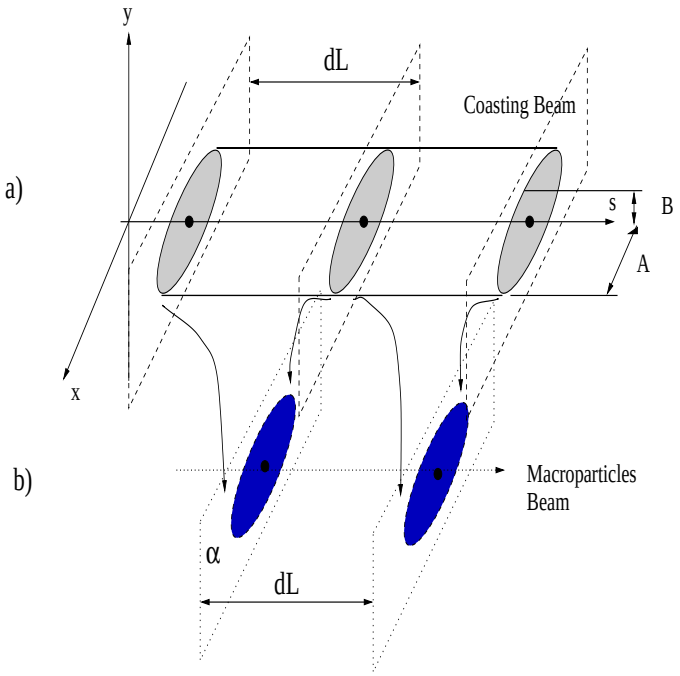

FIGURE 1. Scheme used to introduce the macroparticles description of a coasting beam: the real beam is represented by a macroparticle distribution on a series of transverse planes separated by an axial distance dL.

and $\lambda = x^2/(a_x^2+s) + y^2/(a_y^2+s)$ with $u = x, y$. To evaluate the integral in Eq. (8) we, analogously to a previous bunched beam analysis [5], employ the change of variables $s = \alpha^2(1/u^2 - 1)$, where $\alpha = (a_x a_y)^{1/3}$. Then E_x, for instance, becomes

$$E_x = \frac{q^*}{2\epsilon_0} x \int_0^1 \frac{n(\phi) 2u^2 du}{[(\frac{a_x^2}{\alpha^2} - 1)u^2 + 1]^{3/2} [(\frac{a_y^2}{\alpha^2} - 1)u^2 + 1]^{1/2}} \tag{9}$$

Following [5,6], we expand $n(\phi)$ in a Fourier series as

$$n(\phi) = \frac{c_0}{2} + \sum_{\ell=1}^{\infty} c_\ell \cos\left(\frac{\ell\pi\phi}{\Phi}\right)$$

where

$$c_\ell = \frac{2}{\Phi} \int_0^\Phi n(\phi) \cos\left(\frac{\ell\pi\phi}{\Phi}\right) d\phi \tag{10}$$

and Φ is the maximum value of ϕ (i.e. $n(\Phi) = 0$ defines the beam edge). The relation between the volume of the radial shell where $\phi \in [\phi_i, \phi_i + \Delta\phi]$ and the number of macroparticles ΔN contained within the shell is

$$\frac{\Delta N}{\pi a_x a_y dL} = n(\phi_i)\Delta\phi$$

It is straightforward to see that c_ℓ can be expressed as

$$c_\ell = \frac{2}{\Phi \pi a_x a_y dL} \sum_{i=1}^{N^*} \cos\left(\frac{\ell\pi\phi_i}{\Phi}\right)$$

If we substitute the expansion for $n(\phi)$ in Eq. (9), we can express the electric field, for instance E_x, as

$$E_x = \frac{c_0}{2} F_0^x(x,y,z) + \sum_{\ell=1}^{\infty} c_\ell F_\ell^x(x,y,z) \tag{11}$$

where $F_\ell^x(x,y,z) = x M_x q_x^*/\epsilon_0$ and M_x is given by Eq. (9) with the density n replaced by $\cos(\ell\pi\phi/\Phi)$.

This method of describing the particle density as smooth distribution can represent the electrostatic field produced an arbitrary transverse density profile that is constant on elliptical surfaces.

C Space Charge and Difference Resonances

When there is coupling between the transverse equantions of motion, the space-charge ellipse of the coasting beam can be rotated about the longitudinal axis.

Such coupling can be produced by skew quardupoles and enhance various resonance effects. The rotation angle α of the space-charge ellipse is function of the longitudinal coordinate s. In this case, we can employ the previous technique to calculate the space charge through an appropriate symmetry transformation. The coordinate of a particle $\mathbf{x} = (x, y)$ in the laboratory frame is rotated back by an angle α to $\tilde{\mathbf{x}} = (\tilde{x}, \tilde{y}) = R(-\alpha)\mathbf{x}$, where $\tilde{x}, \tilde{y}$ are the coordinates in the rotated frame. The space charge is then computed for the untilted ellipse in the rotated frame and then transformed back to the laboratory frame. If $\tilde{\mathbf{E}}(\mathbf{x})$ is the electric field for the untilted ellipse in the rotated frame, then the laboratory frame electric field is given by

$$\mathbf{E}(\mathbf{x}) = R(\alpha)\tilde{\mathbf{E}}(R(-\alpha)\mathbf{x})$$

where $R(\alpha)$ denotes a counter-clockwise rotation by angle α. To determine the tilting angle α from the spatial particle distribution, we use the fact that the quantity $\overline{xy} = 0$ in the rotated frame. The condition $\overline{\tilde{x}\tilde{y}} = \overline{(x\cos\alpha - y\sin\alpha)(x\sin\alpha + y\cos\alpha)} = 0$ leads to the equation

$$-m^2\overline{xy} + m(\overline{x^2} - \overline{y^2}) - \overline{xy} = 0$$

where $m = \tan\alpha$. Solving this quadratic equation for m then determines α. The precision of this method in evaluating m depends of the number of macroparticles, the tilting angle α, and the ratio a_x/a_y. If $a_x/a_y \simeq 1$, the relative error of m is large. Hence we take $m = 0$ when the correlation coefficient $\sigma = \overline{xy}^2/(\overline{x^2} \cdot \overline{y^2})$ satisfies $\sigma < 0.2$.

III EMITTANCE EXCHANGE WITH SPACE CHARGE

One limitation of multiturn injection schemes [7,8] is the loss of particles hitting the vertical septum. A skew quadrupole couples the transverse planes exciting a difference resonance. When the bare tune is on such a resonance, horizontal oscillation energy is transfered to the vertical plane and the horizontal amplitude of the injected particle will diminish during the few revolutions of the multiturn injection. This effect can be exploited to move particles away from the septum, thereby improving the injection efficiency.

The single particle dynamics nearby a skew quadrupole driven resonance will be analyzed in sections B and C. When a coasting beam is considered, space charge can be important for the single particle dynamics since it changes the single particle tunes. Since the bandwidth of the resonance can be small, space charge can be a significant effect: the amplitude of exchange and the period of exchange is strongly dependent on the location of the single particle tunes with respect the resonance. As a consequence, the evolution of the emittance exchange is not similar to that of a single particle evolving in the external focusing fields. If the current is strong enough, space charge can push the single particle tunes out of the resonance and suppress the exchange process.

A Lattice Used

The SIS (SchwerIonen-Synchrotron) is a 18 Tesla-meter fast cycling synchrotron that can be used to accelerate a variety of ions. The SIS [2] has a strictly periodic lattice with 12 identical cells. The ion beam is injected at 11.4 MeV/u and a triplet focusing system is employed in each cell. A skew quadrupole scheme is under consideration in the SIS to improve the injection efficiency. We will consider a beam of U^{+28} with $\epsilon_x = 200$ mm mrad and $\epsilon_y = 20$ mm mrad. The emittance exchange is expected to take ~ 30 turns. We have introduced a thin skew quadrupole in the SIS lattice in order to simulate a real skew quadrupole. The skew quadrupole is located at the beginning of the second cell.

B Single Particle Emittance Exchange

As reported in [9], if the bare tunes are on a difference resonance ($q_x - q_y = k - \delta$ with k integer and $\delta << 1$) and if the initial vertical emittance is zero, then the emittances exchange is described by the formula

$$\epsilon_x = \epsilon_{x_0} - \frac{4Q_c^2 \sin^2 \Theta}{\delta^2 + 4Q_c^2}\epsilon_{x_0} \tag{12}$$

Here,

$$\Theta = 2\pi q_x N_t \sqrt{\frac{\delta^2}{4} + Q_c^2} \tag{13}$$

and

$$\epsilon_x + \epsilon_y = const$$

with initial values $\epsilon_{x,0}$ and $\epsilon_{y,0} = 0$, where ϵ_x, ϵ_y are the instantaneous Courant Snyder invariants, Q_c is proportional to the strength of the skew, and N_t is the number of turns.

Eq. (12) shows the mechanism for the emittance exchange: when the initial vertical emittance is zero, ϵ_x is oscillating and the exchange is due to the preservation of $\epsilon_x + \epsilon_y$. On the other hand, Eq. (12) was derived by neglecting second-order derivatives in the equation of motion and assumes only slowly varying amplitudes. These assumptions are strongly related to the strength of the skew: if we require a fast exchange they are not satisfied and the evolution of the Courant Snyder emittances can differ from Eq. (12). For instance, single particle simulations showed that $\epsilon_x + \epsilon_y$ can exhibit a dependence on the longitudinal position (Fig. 2a). However in spite of this difference, simulations indicate that even for a strong skew strength, the $\sin^2$-like evolution of the Courant Snyder emittance predicted by Eq. (12) is still present besides a modulation. Thus it makes sense to consider the amplitude and the period of emittance exchange. Some simulations indicate that an integrated gradient of $j = 0.01$ m^{-1} leads to an emittance exchange in 25 turns. Such a simulated exchange is plotted in Fig. 2b.

C Resonance Bandwidth

In this section we present how the evolution of the emittances can change as function of the tunes. with space-charge neglected. Fig. 2b shows the definition of the amplitude and period of the emittance exchange for a single particle. The discontinuities in the second-derivative of the curve are due to the strong skew kick experienced each turn. Fig. 3 summarizes the simulated behaviour of a single particle near the resonance. In Fig. 3 we have taken 40 working points on a line orthogonal to the resonance $q_x - q_y = 1$ with $q_x = 4.29$ and $q_y = 3.29$. For each working point we determined $\epsilon_{x,max}$ and $\epsilon_{x,min}$ by tracking a particle with initial coordinates $\hat{x} = \sqrt{\epsilon_x}, \hat{p}_x = 0$, and $\hat{y} = \sqrt{\epsilon_y}, \hat{p}_y = 0$ ($\hat{}$ = Courant Snyder coordinates) for 2000 turns. The exchange amplitude was calculated as $\Delta\epsilon_x = \epsilon_{x,max} - \epsilon_{x,min}$ (Fig. 3a,c). The period of the exchange T was computed as follows. 20000 turns were simulated using the same initial condition and measuring (in turns) the position when the instantaneous emittance ϵ_x crosses the average emittance $(\epsilon_{x,max} + \epsilon_{x,min})/2$. All these crossings were used to determined a series of periods from which the average period T was calculated (Fig. 3b,d). When the particle is exactly on the resonance, the linear coupling allows a periodic exchange of energy between the two planes. As the particle moves from the resonance at $q_x = 4.29$, the difference in phase between the horizontal and vertical oscillations reduces the time in which the exchange acts in one direction. This change reduce both the amplitude and period of exchange. The peak near $q_x = 4.5$ in Fig. 3a,b shows a higher order effect.

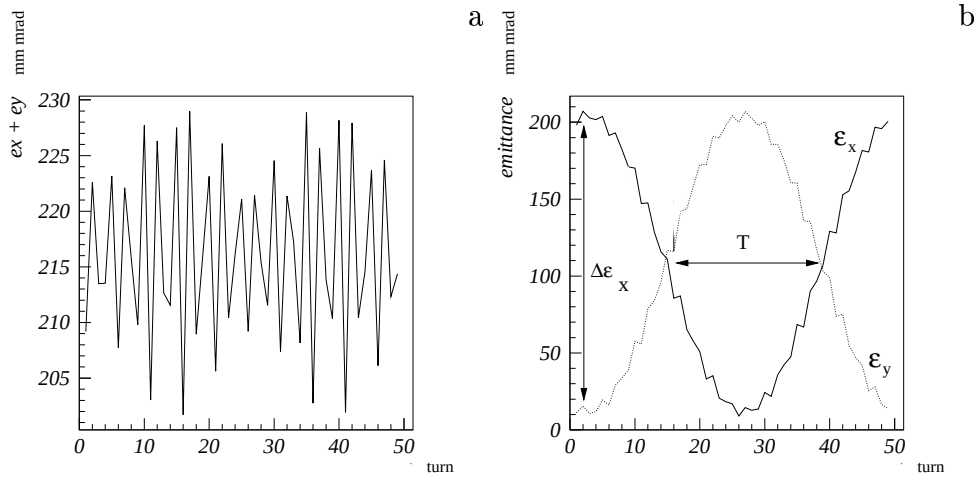

FIGURE 2. Simulated single-particle emittance exchange. a) the sum of the $x-$ and $y-$ emittances is not conserved; b) definition of amplitude and frequency of emittance exchange.

D Simulations of a Coasting Beam on Resonance

We employed the micromap technique to simulate the evolution of a coasting beam in the presence of space charge with an initial transverse K-V distribution. Simulations were carried out with $\delta p = 0$ and for currents of $I = 20$ mA and $I = 140$ mA. 1000 macroparticles were used and the space charge was calculated up to the 5th order (i.e., in Eq. (11) the sum is cut off for $\ell > 5$). The bare tunes of the machine were chosen to lie exactly on a $q_x - q_y = 1$ resonance with $q_x = 4.29$ and $q_y = 3.29$. The time step was chosen to correspond to a longitudinal increment of 1/20 of an SIS cell, i.e. $\Delta t = 0.02$ μs. In Figs. 4a,b,c,d are plotted the horizontal and vertical rms emittances ($\epsilon_{x\ rms}$ and $\epsilon_{y\ rms}$) and beam sizes (x_{rms} and y_{rms}). The discontinuity between the short horizontal lines in Figs. 4c,d show the effect of the skew quadrupole kick, which reaches its maximum strength when $\epsilon_x \simeq \epsilon_y$. The evolution in the rms beam sizes is driven by the emittance exchange. In Figs.

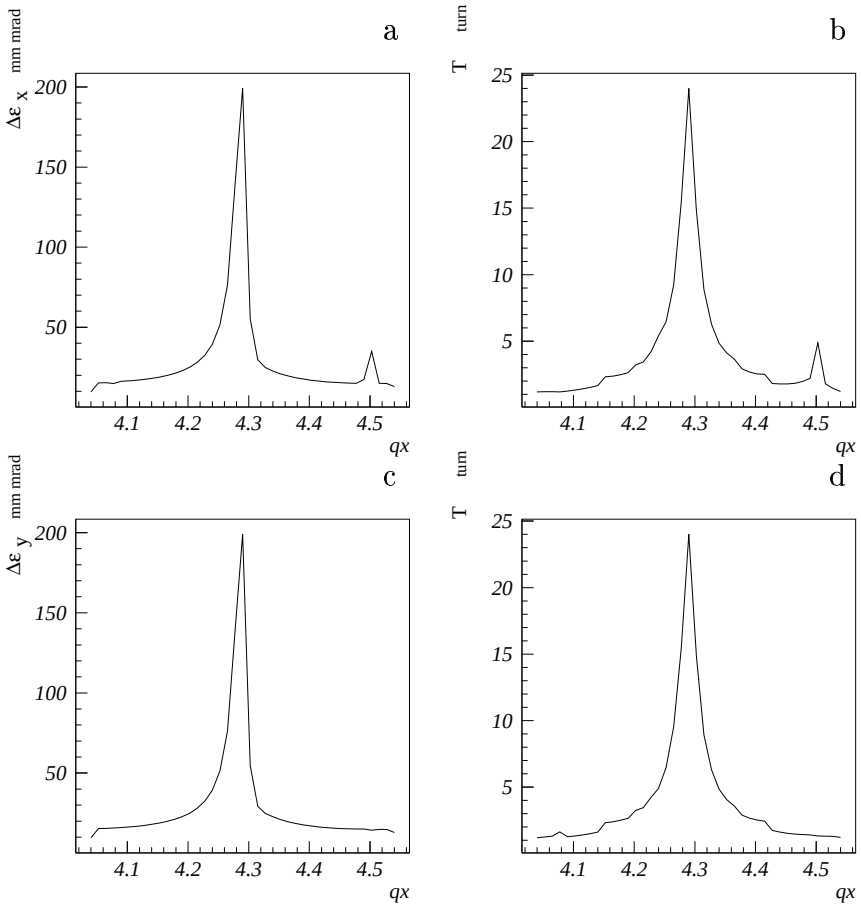

FIGURE 3. a) Amplitude and period of emittance oscillations as a function of q_x. b) Period of ϵ_x oscillation; c) ϵ_y oscillation amplitude; d) Period ϵ_y oscillation.

4a,b the thickness of the band of x_{rms} and y_{rms} values is due to the time step: since Δt is small with respect the time needed to go through one cell, the rms size shows envelope oscillations which when plotted in discrete time intervals look like a band rather than a continuous line. For $I = 20$ mA the initial tuneshifts due to the space charge are $\Delta q_x = -0.0049$ and $\Delta q_y = -0.0178$, so that the tunes of each particle are still near resonance (see Fig. 3) and then a complete rms emittance exchange occurs in 25 turns. Each particle "exchange" starts from different initial conditions, but the evolution of the rms emittances preserve the quantity $\epsilon_{x,rms} + \epsilon_{y,rms}$ better than for the single particle emittances (Fig. 2a). Figs. 5 shows results of a simulation repeated for a current of $I = 140$ mA, with initial tuneshifts of $\Delta q_x = -0.034$ and $\Delta q_y = -0.12$, which brings the single particle tunes to the border of the resonance. In this case the "exchange" is weaker but not as much as indicated by the single particle results in Fig. 3: The exchange period T is reduced to ~ 22 turns and $\Delta\epsilon_x = \Delta\epsilon_y = 80$ mm mrad, while from Fig. 3 we would expect that $\Delta\epsilon_x = \Delta\epsilon_y = 40$ mm mrad and $T = 4$ turns. This decreased exchange rate stems from the collective motion driven by the skew and a coherent effect of the space charge. In fact the skew quadrupole causes the emittance exchange that in turn induces a variation in the single particle tunes through the resonance, causing a partial sampling of the resonance. Figs. 3b,d show that the wave number Θ/N_t of the exchange function in Eq. (13) depends on the single particle tune. Therefore, the phase advance results from the integration of the wave number over the number of turns. In order to have half emittance oscillation, the (phase advance $= \pi$) we need more turns since T is not constant. An analogous argument can be used to explain the larger amplitude of emittance exchange obtained in Fig. 5 with respect the 40 mm mrad predicted in Figs. 3a,c. In these simulations were also included the coherent tuneshift which could be relevant in the exchange process.

IV CONCLUSION

We presented a micromap technique as an extension of a standard transfer map to include space charge defocusing forces for a coasting beam. A macroparticle model was developed to calculate the space charge forces under the assumption of elliptic beam symmetry. A code employing this procedure was written and used to study emittance exchange driven by a skew quadrupole. Results provide evidence of a coherent effect of space charge which improves the exchange with respect the single particle exchange in the absence of space charge. This improvement stems from the coherent motion of the beam. More detailed simulations are needed to investigate this process when the working point of the machine doesn't lie near a resonance and when non-K-V distributions are used to model the initial particle distribution of the beam.

ACKNOWLEDGMENTS

The authors have benefitted from critical comments by Steve Lund.

REFERENCES

1. A. Bazzani, E. Todesco, G. Turchetti and G. Servizi, *A Normal Form Approach to the Theory of Nonlinear Betatronic Motion*, CERN **94-02**, (1994).
2. B. Franczak, GSI-SIS-TN / 87-13, 10. Sept. 1987
3. J. Rossbach and P. Schmüser, *Basic Course on Accelerator optics*, Cern Accelerator School **94 - 01** (1994);
4. F. J. Sacherer, *IEEE Trans. Nucl. Sci.* **NS-18**, 1105 (1971);

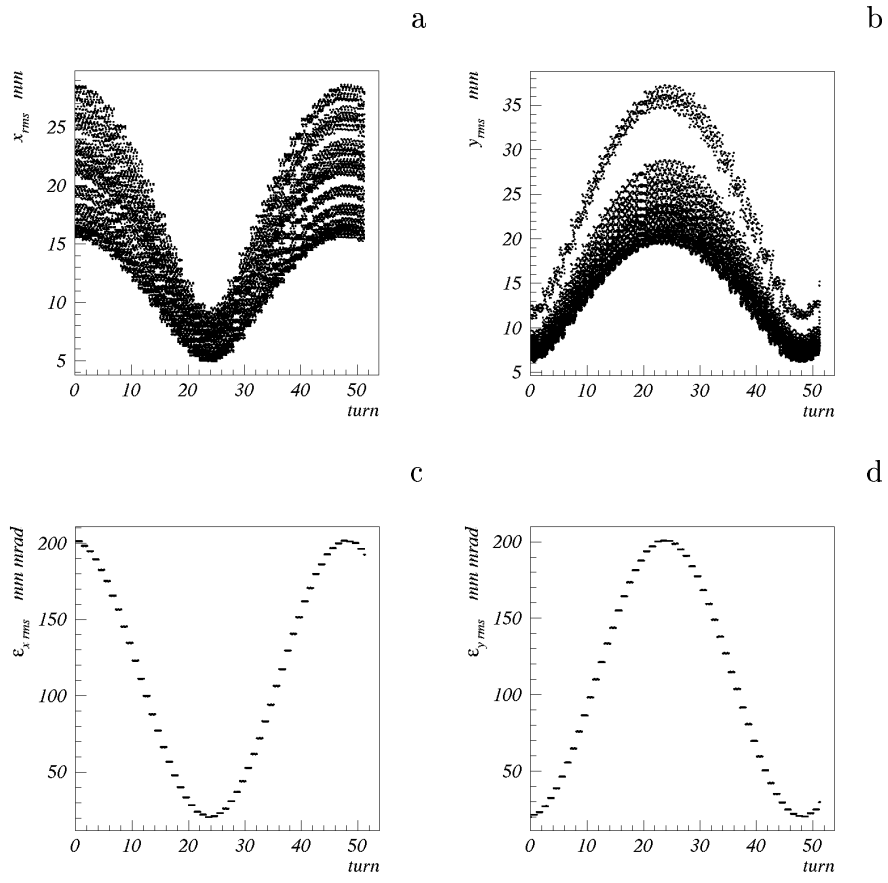

FIGURE 4. Simulated multi-particle evolutions as a function of turn number for I=20 mA a) and b) rms sizes; c) and d) rms emittances.

5. G. Franchetti, I. Hofmann and G. Turchetti *Six-dimensional approach to the beam dynamics in HIDIF scenario.*, Proc. of the 12th Int. Symp. on Heavy Ion Inertial Fusion, Heidelberg (Germany), Sept. 24-27, 1997, to be pubblished on Nuclear Instruments and Methods A;
6. R.W. Garnett and T.P. Wangler, IEEE Particle Accelerator Conference, San Francisco, CA, May 6-9, 1991, IEEE, New York, p. 330.
7. R.W. Hasse and I. Hofmann, *Space charge limit of multiturn injection in HIDIF by 2D and 3D PIC simulation*, Proc. of the 12th Int. Symp. on Heavy Ion Inertial Fusion, Heidelberg (Germany), Sept. 24-27, 1997, to be published on Nuclear Instruments and Methods A;
8. C. Prior and G. Rees, *Multiturn Injection and Lattice Design for HIDIF*, Proc. of the 12th Int. Symp. on Heavy Ion Inertial Fusion, Heidelberg (Germany), Sept. 24-27, 1997, to be published on Nuclear Instruments and Methods A;
9. K. Schindl and P. Van der Stock, *IEEE Trans. Nucl. Sci.* **NS-24**, 1390 (1977).

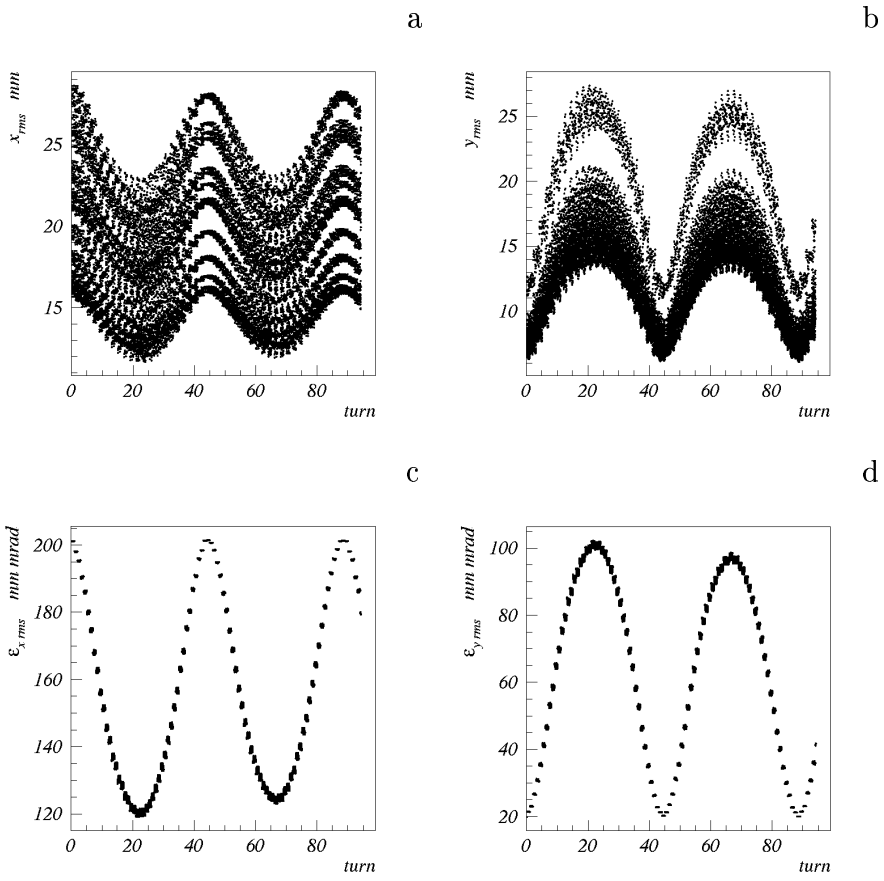

FIGURE 5. Simulated multi-particle evolutions as a function of turn number for I=140 mA a) and b) rms sizes; c) and d) rms emittances.